Charged-particle multiplicity fluctuations in Pb–Pb collisions at √sNN = 2.76 TeV

(ALICE Collaboration) Acharya, S.; ...; Erhardt, Filip; ...; Gotovac, Sven; ...; Jerčić, Marko; ...; Karatović, David; ...; ...

Source / Izvornik: **The European Physical Journal C, 2021, 81**

Journal article, Published version
Rad u časopisu, Objavljena verzija rada (izdavačev PDF)

https://doi.org/10.1140/epjc/s10052-021-09784-4

Eur. Phys. J. C (2021) 81:1012
https://doi.org/10.1140/epjc/s10052-021-09784-4

THE EUROPEAN PHYSICAL JOURNAL C

Regular Article - Experimental Physics

Charged-particle multiplicity fluctuations in Pb–Pb collisions at $\sqrt{s_{\mathrm{NN}}}$ = 2.76 TeV

ALICE Collaboration[⋆]

CERN, 1211 Geneva 23, Switzerland

Received: 27 May 2021 / Accepted: 29 October 2021 / Published online: 17 November 2021

Abstract Measurements of event-by-event fluctuations of charged-particle multiplicities in Pb–Pb collisions at $\sqrt{s_{\mathrm{NN}}} = 2.76$ TeV using the ALICE detector at the CERN Large Hadron Collider (LHC) are presented in the pseudorapidity range $|\eta| < 0.8$ and transverse momentum $0.2 < p_{\mathrm{T}} < 2.0$ GeV/c. The amplitude of the fluctuations is expressed in terms of the variance normalized by the mean of the multiplicity distribution. The η and p_{T} dependences of the fluctuations and their evolution with respect to collision centrality are investigated. The multiplicity fluctuations tend to decrease from peripheral to central collisions. The results are compared to those obtained from HIJING and AMPT Monte Carlo event generators as well as to experimental data at lower collision energies. Additionally, the measured multiplicity fluctuations are discussed in the context of the isothermal compressibility of the high-density strongly-interacting system formed in central Pb–Pb collisions.

1 Introduction

According to quantum chromodynamics (QCD), at high temperatures and high energy densities, nuclear matter undergoes a phase transition to a deconfined state of quarks and gluons, the quark–gluon plasma (QGP) [1–5]. Heavy-ion collisions at ultra-relativistic energies make it possible to create and study such strongly-interacting matter under extreme conditions. The QGP formed in high-energy heavy-ion collisions has been characterised as a strongly-coupled system with very low shear viscosity. The primary goal of the heavy-ion program at the CERN Large Hadron Collider (LHC) is to study the QCD phase structure by measuring the properties of QGP matter. One of the important methods for this study is the measurement of event-by-event fluctuations of experimental observables. These fluctuations are sensitive to the proximity of the phase transition and thus provide information on the nature and dynamics of the system formed in the collisions [6–12]. Fluctuation measurements provide a powerful tool to investigate the response of a system to external perturbations. Theoretical developments suggest that it is possible to extract quantities related to the thermodynamic properties of the system, such as entropy, chemical potential, viscosity, specific heat, and isothermal compressibility [6,13–21]. In particular, isothermal compressibility expresses how a system's volume responds to a change in the applied pressure. In the case of heavy-ion collisions, it has been shown that the isothermal compressibility can be calculated from the event-by-event fluctuation of charged-particle multiplicity distributions [17].

The measured multiplicity scales with the collision centrality in heavy-ion collisions. The distribution of particle multiplicities in a given class of centrality and its fluctuations on an event-by-event basis provide information on particle production mechanisms [22–24]. In this work, the magnitude of the fluctuations is quantified in terms of the scaled variance,

$$\omega_{\mathrm{ch}} = \frac{\sigma_{\mathrm{ch}}^2}{\langle N_{\mathrm{ch}} \rangle}, \tag{1}$$

where $\langle N_{\mathrm{ch}} \rangle$ and σ_{ch}^2 denote the mean and variance of the charged-particle multiplicity distribution, respectively. Event-by-event multiplicity fluctuations in heavy-ion collisions have been studied earlier at the BNL-AGS by E802 [25], the CERN-SPS by the WA98 [26], NA49 [27,28], and CERES [29] experiments, and at the Relativistic Heavy Ion Collider (RHIC) by the PHOBOS [30] and PHENIX [31] experiments. A compilation of available experimental data and comparison to predictions of the event generators are presented elsewhere [19]. In this work, measurements of the scaled variance of multiplicity fluctuations are presented as a function of collision centrality in Pb–Pb collisions at $\sqrt{s_{\mathrm{NN}}} = 2.76$ TeV using the ALICE detector at the LHC.

In thermodynamics, the isothermal compressibility (k_T) is defined as the fractional change in the volume of a system with change of pressure at a constant temperature,

$$k_T = -\frac{1}{V}\left(\frac{\partial V}{\partial P}\right)\bigg|_T, \tag{2}$$

⋆ e-mail: alice-publications@cern.ch

where V, T, P are the volume, temperature, and pressure of the system, respectively. In general, an increase in the applied pressure leads to a decrease in volume, so the negative sign makes the value of k_T positive. In the context of a description in terms of the grand canonical ensemble, which is approximately applicable for the description of particle production in heavy-ion collisions [5], the scaled variance of the multiplicity distribution can be expressed as [17],

$$\omega_{\mathrm{ch}} = \frac{k_{\mathrm{B}} T \langle N_{\mathrm{ch}} \rangle}{V} k_T, \tag{3}$$

where k_{B} is the Boltzmann's constant, and $\langle N_{\mathrm{ch}} \rangle$ is the average number of charged particles. Measurements of fluctuations in terms of ω_{ch} can be exploited to determine k_T and associated thermodynamic quantities such as the speed of sound within the system [17,32].

Measurements of the multiplicity of produced particles in relativistic heavy-ion collisions are basic to most of the studies as a majority of the experimentally observed quantities are directly related to the multiplicity. The variation of the multiplicity depends on the fluctuations in the collision impact parameter or the number of participant nucleons. Thus, the measured multiplicity fluctuations contain contributions from event-by-event fluctuations in the number of participant nucleons, which forms the main background towards the evaluation of any thermodynamic quantity [33,34]. This has been partly addressed by selecting narrow intervals in centrality and accounting for the multiplicity variation within the centrality of the measurement. The remainder of participant fluctuations is estimated in the context of an MC Glauber model in which nucleus–nucleus collisions are considered to be a superposition of nucleon–nucleon interactions.

Thus, the background fluctuations contain contributions from independent particle production and correlations corresponding to different physical origins. The background-subtracted fluctuations can be used in Eq. (3) to estimate k_T with the knowledge of the temperature and volume from complementary analyses of hadron yields, calculated at the chemical freeze-out [35,36].

In addition to fluctuations in the number of participant nucleons, several other processes contribute to fluctuations of the charged particles multiplicity on an event-by-event basis [17,37]. These include long-range particle correlations, charge conservation, resonance production, radial flow, as well as Bose–Einstein correlations. Since these contributions can not be evaluated directly, the value of k_T extracted and reported in this work amounts to an upper limit.

The article is organized as follows. In Sect. 2, the experimental setup and details of the data analysis method, including event selection, centrality selection, corrections for finite width of the centrality intervals, and particle losses are presented. In Sect. 3, the measurements of the variances of multiplicity distributions are presented as a function of collision centrality. Additionally, the dependence of the fluctuations on the η and p_{T} ranges of the measured charged hadrons are studied. The results are compared with calculations from selected event generators. In Sect. 4, methods used to estimate multiplicity fluctuations resulting from the fluctuations of the number of participants are discussed. An estimation of the isothermal compressibility for central collisions is made in Sect. 5.

2 Experimental setup and analysis details

The ALICE experiment [38] is a multi-purpose detector designed to measure and identify particles produced in heavy-ion collisions at the LHC. The experiment consists of several central barrel detectors positioned inside a solenoidal magnet operated at 0.5 T field parallel to the beam direction and a set of detectors placed at forward rapidities. The central barrel of the ALICE detector provides full azimuthal coverage for track reconstruction within a pseudorapidity (η) range of $|\eta| < 0.8$. The Time Projection Chamber (TPC) is the main tracking detector of the central barrel, consisting of 159 pad rows grouped into 18 sectors that cover the full azimuth. The Inner Tracking System (ITS) consists of six layers of silicon detectors employing three different technologies. The two innermost layers are Silicon Pixel Detectors (SPD), followed by two layers of Silicon Drift Detectors (SDD), and finally, the two outermost layers are double-sided Silicon Strip Detectors (SSD). The V0 detector consists of two arrays of scintillators located on opposite sides of the interaction point (IP). It features full azimuthal coverage in the forward and backward rapidity ranges, $2.8 < \eta < 5.1$ (V0A) and $-3.7 < \eta < -1.7$ (V0C). The V0 detectors are used for event triggering purposes as well as to evaluate the collision centrality on an event-by-event basis [39]. The impact of the detector response on the measurement of charged-particle multiplicity based on Monte Carlo simulations is studied with the GEANT3 framework [40].

This analysis is based on Pb–Pb collision data recorded in 2010 at $\sqrt{s_{\mathrm{NN}}} = 2.76$ TeV with a minimum-bias trigger comprising of a combination of hits in the V0 detector and the two innermost (pixel) layers of the ITS. In total, 13.8 million minimum-bias events satisfy the event selection criteria. The primary interaction vertex of a collision is obtained by extending correlated hits in the two SPD layers to the beam axis. The longitudinal position of the interaction vertex in the beam (z) direction (V_z) is restricted to $|V_z| < 10$ cm to ensure a uniform acceptance in the central η region. The interaction vertex is also obtained from TPC tracks. The event selection includes an additional vertex selection criterion, where the difference between the vertex using TPC tracks and the vertex using the SPD is less than 5 mm in the z-direction. This selection criterion greatly suppresses the contamination of the primary tracks by secondary tracks resulting from weak decays and spurious interactions of particles within the apparatus.

Charged particles are reconstructed using the combined information of the TPC and ITS [38]. In the TPC, tracks are reconstructed from a collection of space points (clusters). The selected tracks are required to have at least 80 reconstructed space points. Different combinations of tracks in the TPC and SPD hits are utilized to correct for detector acceptances and efficiency losses. To suppress contributions from secondary tracks (i.e., charged particles produced by weak decays and interactions of particles with materials of the detector), the analysis is restricted to charged-particle tracks featuring a distance of closest approach (DCA) to the interaction vertex, $\mathrm{DCA_{xy}} < 2.4$ cm in the transverse plane and of $\mathrm{DCA_z} < 3.2$ cm along the beam direction. The tracks are additionally restricted to the kinematic range, $|\eta| < 0.8$ and $0.2 < p_\mathrm{T} < 2.0$ GeV/c.

2.1 Centrality selection and the effect of finite width of the centrality intervals

The collision centrality is estimated based on the sum of the amplitudes of the V0A and V0C signals (known as the V0M collision centrality estimator) [39]. Events are classified in percentiles of the hadronic cross section using this estimator. The average number of participants in a centrality class, denoted by N_part, is obtained by comparing the V0M multiplicity to a geometrical Glauber model [41]. Thus, the centrality of the collision is measured based on the V0M centrality estimator, whereas the measurement of multiplicity fluctuations is based on charged particles measured within the acceptance of the TPC.

A given centrality class is a collection of events of measured multiplicity distributions within a range in V0M corresponding to a mean number of participants, $\langle N_\mathrm{part}\rangle$. This results in additional fluctuations in the number of particles within each centrality class. To account for these fluctuations, a centrality interval width correction is employed. The procedure involves dividing a broad centrality class into several narrow intervals and correcting for the finite interval using weighted moments according to [42,43],

$$X = \frac{\sum_\mathrm{i} n_\mathrm{i} X_\mathrm{i}}{\sum_\mathrm{i} n_\mathrm{i}}. \tag{4}$$

Here, the index i runs over the narrow centrality intervals. X_i and n_i are the corresponding moments of the distribution and number of events in the ith interval, respectively. With this, one obtains, $N = \sum_\mathrm{i} n_\mathrm{i}$ as the total number of events in the broad centrality interval.

The centrality resolution of the combined V0A and V0C signals ranges from 0.5% in central to 2% in the most peripheral collisions [39]. A correction for the finite width of centrality intervals has been made with Eq. 4 using 0.5% centrality intervals from central to 40% cross-section and 1% intervals for the rest of the centrality classes.

2.2 Efficiency correction

The detector efficiency factors (ε) were evaluated in bins of pseudorapidity η, azimuthal angle φ, and p_T. By defining $N_\mathrm{ch}(x)$ as the number of produced particles in a phase-space bin at x, $n(x)$ as the number of observed particles at x, and $\varepsilon(x)$ as the detection efficiency, the first and second factorial moments of the multiplicity distributions can be corrected for particle losses according to the procedure outlined in Refs. [44,45]:

$$F_1 = \langle N_\mathrm{ch}\rangle = \sum_{i=1}^{m}\langle N_\mathrm{ch}(x_\mathrm{i})\rangle = \sum_{i=1}^{m}\frac{n(x_\mathrm{i})}{\varepsilon(x_\mathrm{i})}, \tag{5}$$

and

$$F_2 = \sum_{i=1}^{m}\sum_{j=i}^{m}\frac{\langle n(x_\mathrm{i})(n(x_\mathrm{j}) - \delta_{x_\mathrm{i}x_\mathrm{j}}))\rangle}{\varepsilon(x_\mathrm{i})\varepsilon(x_\mathrm{j})}, \tag{6}$$

respectively. Here, m denotes the index of the phase-space bins and i, j are the bin indexes. $\delta_{x_\mathrm{i}x_\mathrm{j}} = 1$ if $x_\mathrm{i} = x_\mathrm{j}$ and zero otherwise. The variance of the charged-particle multiplicity is then calculated as:

$$\sigma^2_\mathrm{ch} = F_2 + F_1 - F_1^2. \tag{7}$$

The correction procedure is validated by a Monte Carlo study employing two million Pb–Pb events at $\sqrt{s_\mathrm{NN}} = 2.76$ TeV generated using the HIJING event generator [46], and passed through GEANT3 simulations of the experimental setup, taking care of the acceptances of the detectors. The efficiency dependencies on η, φ, and p_T are calculated from the ratio of the number of reconstructed charged particles by the number of produced particles. In order to account for the p_T dependence of efficiency, the full p_T range ($0.2 < p_\mathrm{T} < 2.0$ GeV/c) was divided to nine bins (0.2–0.3, 0.3–0.4, 0.4–0.5, 0.5–0.6, 0.6–0.8, 0.8–1.0, 1.0–1.2, 1.2–1.6, 1.6–2.0) with larger number of bins in low p_T ranges. In the Monte Carlo closure test, the values of $\langle N_\mathrm{ch}\rangle$, σ_ch, and ω_ch of the efficiency corrected results from the simulated events are compared to those of HIJING at the generator level to obtain the corrections. By construction, the efficiency corrected values for $\langle N_\mathrm{ch}\rangle$ match with those from the generator, whereas σ_ch and ω_ch values differ by ~ 0.7 and $\sim 1.4\%$, respectively. These differences are included in the systematic uncertainties.

2.3 Statistical and systematic uncertainties

The statistical uncertainties of the moments of multiplicity distributions are calculated based on the method of error

Table 1 Systematic uncertainties on the mean, standard deviation, and scaled variance of charged-particle multiplicity distributions from different sources. The ranges of uncertainties quoted correspond to central to peripheral collisions

Source	$\langle N_{ch} \rangle$	σ_{ch}	ω_{ch}
Track selection	3.5–4.8%	3.8–6.0%	4.0–7.5%
Variation of DCA_{xy}	0.5–0.9%	0.8–1.2%	1.3–1.6%
Variation of DCA_z	0.4–0.9%	0.7–1.0%	1.2–1.7%
Vertex (V_z) selection	0.1–0.5%	0.5%	0.1–0.8%
Removal of V_x, V_y selections	0.1%	0.2%	0.5%
Efficiency correction	$< 0.1\%$	0.7%	1.4%
Magnetic polarity	0.2–1.0%	0.5–1.5%	0.8–1.7%
Total	3.5–5.1%	4.1–6.4%	4.8–8.3%

propagation derived from the delta theorem [47]. The systematic uncertainties have been evaluated by considering the effects of various criteria in track selection, vertex determination, and efficiency corrections.

The systematic uncertainties related to the track selection criteria were obtained by varying the track reconstruction method and track quality cuts. The nominal analysis was carried out with charged particles reconstructed within the TPC and ITS. For systematic checks, the full analysis is repeated for tracks reconstructed using only the TPC information. The differences in the values of $\langle N_{ch} \rangle$, σ_{ch}, and ω_{ch} resulting from the track selections using the two methods are listed in Table 1 as a part of the systematic uncertainties. The DCA_{xy} and DCA_z of the tracks are varied by $\pm 25\%$ to obtain the systematic uncertainties caused by variations in the track quality selections. The effect of the selection of events based on the vertex position is studied by restricting the z-position of the vertex to ± 5 cm from the nominal ± 10 cm, and additionally by removing restrictions on V_x and V_y. The efficiency correction introduces additional systematic uncertainty as discussed earlier. The experimental data were recorded for two different magnetic field polarities. The two data sets are analyzed separately and the differences are taken as a source of systematic uncertainties.

The individual sources of systematic uncertainties discussed above are considered uncorrelated and summed in quadrature to obtain the total systematic errors reported in this work. Table 1 lists the systematic uncertainties associated with the values of $\langle N_{ch} \rangle$, σ_{ch}, and ω_{ch}.

3 Results and discussions

Figure 1 shows the corrected mean ($\langle N_{ch} \rangle$), standard deviation (σ_{ch}), and scaled variance (ω_{ch}) as a function of $\langle N_{part} \rangle$ for the centrality range considered (0-60%) corresponding to $N_{part} > 45$. Uncertainties on the estimated number of participants, $\langle N_{part} \rangle$, obtained from Ref. [38], are smaller than the width of the solid red circles used to present the data in the centrality range considered in this measurement. It is observed that the values of $\langle N_{ch} \rangle$ and σ_{ch} increase with increasing $\langle N_{part} \rangle$. The value of ω_{ch} decreases monotonically by $\sim 29\%$ from peripheral to central collisions.

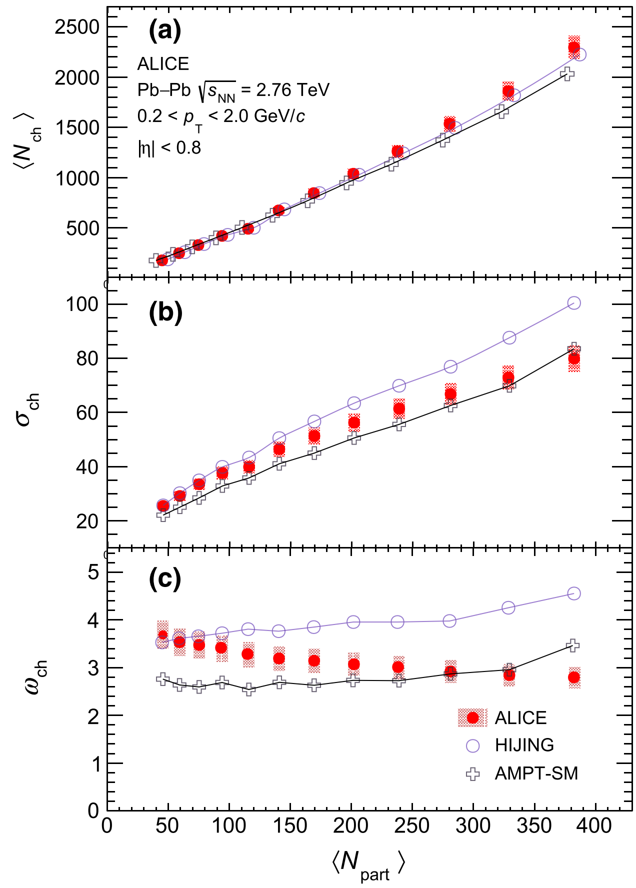

Fig. 1 Mean ($\langle N_{ch} \rangle$), standard deviation (σ_{ch}), and scaled variance (ω_{ch}) of charged-particle multiplicity distributions as a function of the number of participating nucleons for experimental data along with HIJING and AMPT (string melting) models for Pb–Pb collisions at $\sqrt{s_{NN}} = 2.76$ TeV, shown in panels **a**, **b**, and **c**, respectively. For panel **a**, $\langle N_{part} \rangle$ for the two models are shifted for better visibility. The statistical uncertainties are smaller than the size of the markers. The systematic uncertainties are presented as filled boxes

3.1 Comparison with models

The measured ω_{ch} values are compared with the results of simulations with the HIJING and the string melting option of the AMPT models. HIJING [46] is a Monte Carlo event generator for parton and particle production in high-energy hadronic and nuclear collisions and is based on QCD-inspired models which incorporate mechanisms such as multiple minijet production, soft excitation, nuclear shadowing of parton distribution functions, and jet interactions in the

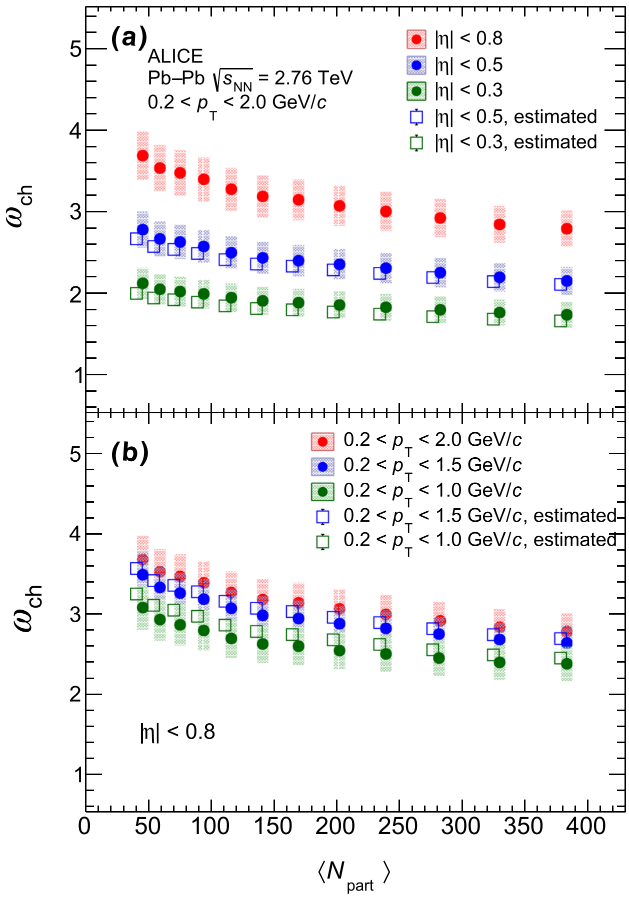

Fig. 2 Scaled variances of charged-particle multiplicity distributions for different η and p_T ranges as a function of number of participating nucleons measured in Pb–Pb collisions at $\sqrt{s_{NN}} = 2.76$ TeV, shown in panels **a**, and **b**, respectively. The estimated ω_{ch} for $|\eta| < 0.3$ and $|\eta| < 0.5$ are obtained from the experimental data of $|\eta| < 0.8$ by using Eq. 8. The estimated ω_{ch} for $0.2 < p_T < 1.5$ GeV/c and $0.2 < p_T < 1.0$ GeV/c are obtained from the experimental data of $0.2 < p_T < 2.0$ GeV/c, also by using Eq. 8. The statistical uncertainties are smaller than the size of the markers. The systematic uncertainties are presented as filled boxes

dense hadronic matter. The HIJING model treats a nucleus-nucleus collision as a superposition of many binary nucleon-nucleon collisions. In the AMPT model [48], the initial parton momentum distribution is generated from the HIJING model. In the default mode of AMPT, energetic partons recombine and hadrons are produced via string fragmentation. The string melting mode of the model includes a fully partonic phase that hadronises through quark coalescence.

In order to enable a proper comparison with data obtained in this work, Monte Carlo events produced with HIJING and AMPT are grouped in collision centrality classes based on generator level charged-particle multiplicities computed in the ranges $2.8 < \eta < 5.1$ and $-3.7 < \eta < -1.7$, corresponding to the V0A and V0C pseudorapidity coverages. The results of the scaled variances from the two event generators are presented in Fig. 1 as a function of the estimated number of participants, N_{part}. As a function of increasing centrality, the ω_{ch} values obtained from the event generators show upward trends, which are opposite to those of the experimental data. It is to be noted that the Monte Carlo event generators are successful in reproducing the mean of multiplicity distributions. This follows from the fact that the particle multiplicities are proportional to the cross sections. On the other hand, the widths of the distributions originate from fluctuations and correlations associated with effects of different origins, such as long-range correlations, Bose–Einstein correlations, resonance decays, and charge conservation. Because of this, the event generators fall short of reproducing the observed scaled variances.

3.2 Scaled variance dependence on pseudorapidity acceptance and p_T range

Charged-particle multiplicity distributions depend on the acceptance of the detection region. Starting with the measured multiplicity fluctuations within $|\eta| < 0.8$ and $0.2 < p_T < 2.0$ GeV/c with a mean $\langle N_{ch}\rangle$ and scaled variance of ω_{ch}, the scaled variance (ω_{ch}^{acc}) for a fractional acceptance in η or for a limited p_T range with mean of $\langle N_{ch}^{acc}\rangle$ can be expressed as [31],

$$\omega_{ch}^{acc} = 1 + f^{acc}(\omega_{ch} - 1), \tag{8}$$

$$\text{where} \quad f^{acc} = \frac{\langle N_{ch}^{acc}\rangle}{\langle N_{ch}\rangle}. \tag{9}$$

This empirical estimation for the acceptance dependence of the scaled variance is valid assuming that there are no significant correlations present over the acceptance range being studied. The validity of this dependence has been checked by comparing the experimental data of scaled variances at reduced acceptances along with the results from the above calculations. This is shown in Fig. 2 for different η or p_T ranges. In the top panel, the scaled variances are shown, as a function of $\langle N_{part}\rangle$, for three η ranges. The solid symbols show the results of measured scaled variances, whereas open symbols show the estimated values for the two reduced η windows. The calculated values yield a good description of the measured data points. The choice of the p_T range also affects the multiplicity of an event. In the bottom panel of Fig. 2, the scaled variances are shown, as a function of $\langle N_{part}\rangle$, for three p_T ranges keeping $|\eta| < 0.8$. A decrease in the value of ω_{ch} is observed with the decrease of the p_T window. The results from the calculations of scaled variances are compared to the measured data points. The calculated values are close to those of the measurement. This estimation of the scaled variances of multiplicity distributions is particularly useful in extrapolating fluctuations to different coverages.

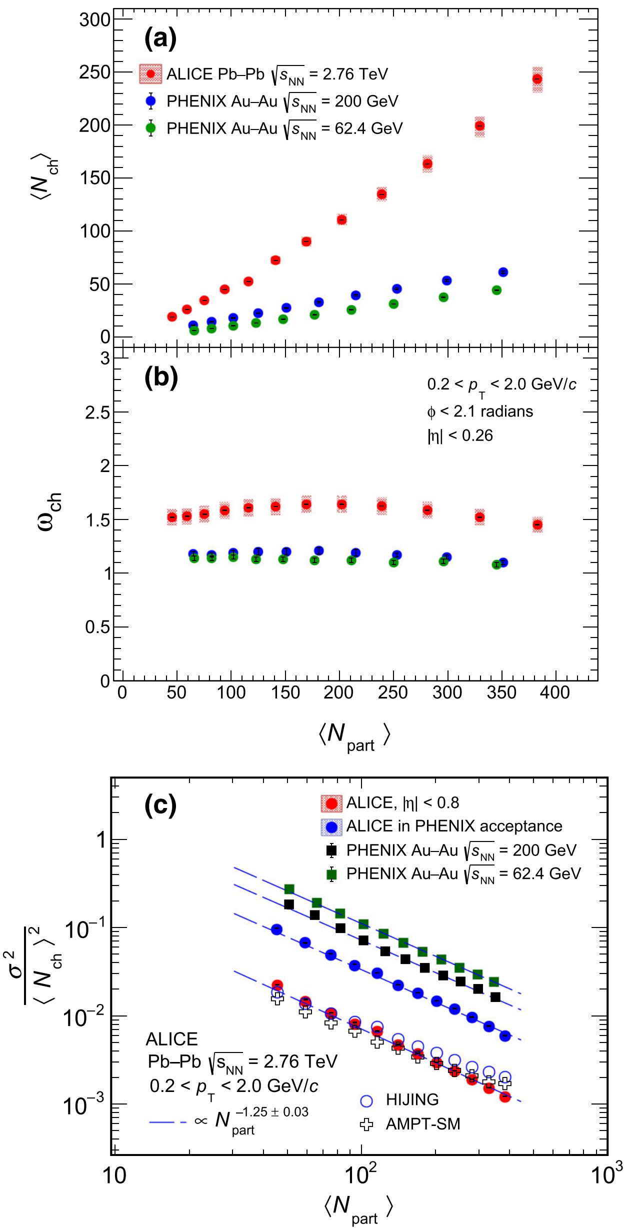

Fig. 3 Comparison of $\langle N_{ch}\rangle$, ω_{ch}, and $\sigma^2_{ch}/\langle N_{ch}\rangle^2$ measured in this work based on the acceptance of the PHENIX experiment with results reported by PHENIX [31] as a function of number of participating nucleons, shown in panels **a**, **b**, and **c**, respectively. The statistical uncertainties are smaller than the size of the markers. The systematic uncertainties are presented as filled boxes

3.3 Comparison to scaled variances at lower collision energies

Scaled variances of charged-particle multiplicity distributions were earlier reported by the PHENIX Collaboration at RHIC for Au–Au collisions at $\sqrt{s_{NN}} = 62.4$ and 200 GeV [31]. The beam–beam counters (BBC) in PHENIX covering the full azimuthal angle in the pseudorapidity range $3.0 < |\eta| < 3.9$ provided the minimum-bias trigger and were used for centrality selection. The pseudorapidity acceptance of the PHENIX experiment amounted to $|\eta| < 0.26$ with an effective average azimuthal active area of 2.1 radian and $0.2 < p_T < 2.0$ GeV/c for charged particle measurements. The published results of mean and scaled variances of charged-particles were corrected for fluctuations of the collision geometry within a centrality bin. This was performed by comparing fluctuations from simulated HIJING events with a fixed impact parameter to events with a range of impact parameters covering the width of the centrality bin, as determined from Glauber model simulations. The corrected results are reproduced in Fig. 3 for the two collision energies. To enable an appropriate comparison with results reported by PHENIX, the ALICE data are reanalyzed by imposing the same kinematic ranges as in PHENIX, and the resulting mean and scaled variances are presented in Fig. 3. It is observed that for the same acceptance and kinematic cuts, the mean values and the scaled variances are larger at the LHC energy compared to those obtained at RHIC energies.

It is also of interest to study $\frac{\sigma^2_{ch}}{\langle N_{ch}\rangle^2}$, the ratio of the variance by the square of the average multiplicity as a function of collision centrality. At lower beam energies, these distributions obey a power-law relative to the number of participants [49]. In the lower panel of Fig. 3, the values of $\frac{\sigma^2_{ch}}{\langle N_{ch}\rangle^2}$ are presented as a function of $\langle N_{part}\rangle$ for the ALICE data, for the common coverage of ALICE and PHENIX data, as well as PHENIX data at two collision energies. The data points are fitted by a scaling curve, $\frac{\sigma^2_{ch}}{\langle N_{ch}\rangle^2} = A \cdot N^{\alpha}_{part}$. The exponent $\alpha = -1.25 \pm 0.03$ fits the four sets of experimental data well with χ^2/ndf (where ndf is the number of degrees of freedom) as 0.88, 1.1, 0.95, 0.84 for Pb–Pb collisions at $\sqrt{s_{NN}} = 2.76$ TeV with the ALICE acceptance, the PHENIX detector acceptance and Au–Au collisions at $\sqrt{s_{NN}} = 200$ GeV and 62.4 GeV, respectively. The scaling, first described by the PHENIX Collaboration [49], also holds for the ALICE data. The corresponding values of $\frac{\sigma^2_{ch}}{\langle N_{ch}\rangle^2}$ for HIJING and AMPT models for Pb–Pb collisions at $\sqrt{s_{NN}} = 2.76$ TeV are also displayed in Fig. 3. The trends as a function of centrality are observed to be similar to those of the experimental data. Fits with a similar scaling curve yield power-law exponents as −1.1 and −1.05 for HIJING and AMPT models, respectively. These exponents for the models are lower compared those of the experimental data.

4 Background to the measured multiplicity fluctuations

The background to the measured multiplicity fluctuations contains contributions from several sources. In this section, the background fluctuations are presented first from a par-

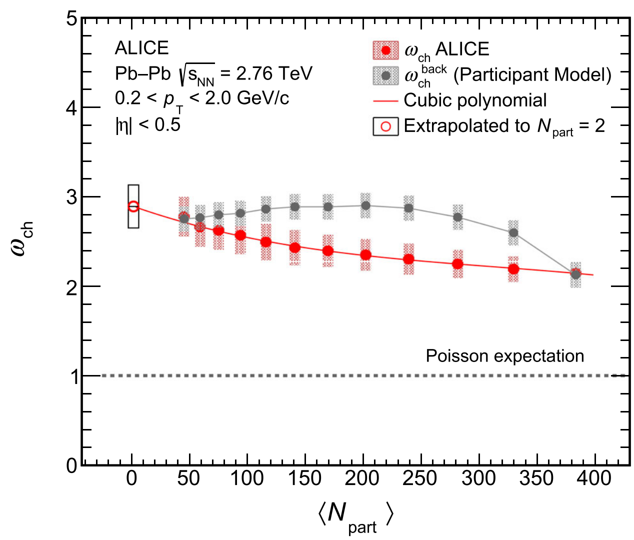

Fig. 4 Scaled variance as a function of $\langle N_{part} \rangle$ for charged-particle multiplicity distributions and background fluctuations (ω_{ch}^{back}) based on a participant model calculation for $|\eta| < 0.5$. The expectation from Poisson-like particle production is indicated by the dotted line. The statistical uncertainties are smaller than the size of the markers. The systematic uncertainties are presented as filled boxes

ticipant model calculation and then the expectations from a Poisson distribution of particle multiplicity are discussed.

In the wounded nucleon model, nucleus–nucleus (such as Pb–Pb) collisions are considered to be a superposition of individual nucleon–nucleon interactions. In this context, the fluctuations in multiplicity within a given centrality window arise in part from fluctuations in N_{part} and from fluctuations in the number of particles (n) produced by each nucleon–nucleon interaction [22,26,31]. The values of n and their fluctuations are also strongly dependent on the acceptance of the detector. Within the context of this framework, the scaled variance of the background, ω_{ch}^{back}, amounts to

$$\omega_{ch}^{back} = \omega_n + \langle n \rangle \omega_{N_{part}}, \tag{10}$$

where $\langle n \rangle$ is the average number of particles produced by each nucleon–source within the detector acceptance, ω_n is the scaled variance of the fluctuations in n, and $\omega_{N_{part}}$ denotes the fluctuations in N_{part}. The variance, $\omega_{N_{part}}$ is calculated using event-by-event N_{part} from the HIJING model. The distribution of N_{part} corresponds to the centrality obtained within the V0 detector coverage ($2.8 < \eta < 5.1$ and $-3.7 < \eta < -1.7$). The extracted values of $\omega_{N_{part}}$ are corrected for the effects of the finite width of the centrality intervals.

For the central rapidity range ($|\eta| < 0.5$), the measured number of charged particles produced in pp collisions within $0.2 < p_T < 2.0$ GeV/c at $\sqrt{s}$ = 2.76 TeV [50] yields $\langle n \rangle = 1.45 \pm 0.07$, which is half of the measured value. In order to calculate ω_n, an extrapolation of the measured ω_{ch} is made to $N_{part} = 2$ using a polynomial fit function of the form $a + bx + cx^2 + dx^3$, which is shown in Fig. 4. In order to calculate ω_n, an extrapolation of the measured ω_{ch} is made to $N_{part} = 2$ using a polynomial fit function of the form $a + bx + cx^2 + dx^3$, which is shown in Fig. 4. Since both the nucleon sources contributing to $N_{part} = 2$ are correlated, ω_n becomes half of the extrapolated value, yielding $\omega_n = 1.445 \pm 0.12$. This result is also consistent with the value of $\omega_n = 1.51 \pm 0.16$ obtained from the parameterization given by the PHENIX Collaboration [31].

Using the above numbers, ω_{ch}^{back} are calculated and plotted as a function of $\langle N_{part} \rangle$ as in Fig. 4. The obtained trend in ω_{ch}^{back} mainly arises from the centrality dependence of $\omega_{N_{part}}$. For most central collisions, the difference between the measured and background ω_{ch} is 0.02 ± 0.18, which is consistent with zero within the uncertainties. Except for most central collisions, ω_{ch}^{back} is observed to be larger than ω_{ch}. Thus, it seems likely that the background estimated in this way from the participant model is overestimated.

For an ideal gas, the number fluctuations are described by the Poisson distribution. So, if the emitted particles are uncorrelated, then the multiplicity distributions become Poissonian, the magnitude of ω_{ch} reduces to unity, which is independent of the multiplicity and thus independent of the centrality of the collision. As seen from Fig. 4, the observed multiplicity fluctuations are significantly above the Poisson expectation for all centralities.

5 Estimation of isothermal compressibility

Equation (3) relates the magnitude of the charged-particle multiplicity fluctuations to the isothermal compressibility. The calculation of k_T requires knowledge of the temperature and volume of the system. After the collision, as the system cools down, the hadronic yields are fixed when the rate of inelastic collisions becomes negligible (chemical freeze-out), but the transverse-momentum distributions continue to change until elastic interactions also cease (kinetic freeze-out). The number of charged particles gets fixed at the time of chemical freeze-out (except for long-lived resonances). As the calculation of k_T depends on the fluctuations in the number of particles, the chemical freeze-out conditions are considered as input. The ALICE Collaboration has published the identified particle yields of pions, kaons, protons, light nuclei, and resonances [36,51,52]. The statistical hadronization models have been successful in describing these yields and their ratios [5,35,53], using temperature and volume as parameters at the chemical freeze-out. For most central Pb–Pb collisions at $\sqrt{s_{NN}} = 2.76$ TeV, the ALICE data on yields of particles in one unit of rapidity at mid-rapidity are in good agreement with 0.156 ± 0.002 GeV and 5330 ± 505 fm^3, for temperature and volume, respectively [52]. In addition, the charged-particle multiplicity within $|\eta| < 0.5$ in this centrality range is $\langle N_{ch} \rangle = 1410 \pm 47$ $(syst)$.

Here, an attempt is made to estimate k_T for Pb–Pb collisions using the charged-particle multiplicity fluctuations along with the temperature, volume, and mean number of charged particles from above. The measured multiplicity fluctuation for central collisions is $\omega_{\mathrm{ch}} = 2.15 \pm 0.1$. In the absence of any background where the full fluctuation is attributed to have a thermal origin, one would obtain $k_T = 52.1 \pm 5.81$ fm^3/GeV. As the measured ω_{ch} contains background fluctuations from different sources, this value of k_T can be only be considered as an absolute upper limit.

In the previous section, the background fluctuations have been estimated from the participant model calculation as shown in Fig. 4. For central collisions, the value of the measured fluctuation above that of the participant model fluctuation is $\omega_{\mathrm{ch}} = 0.02 \pm 0.18$. This leads to $k_T = 0.48 \pm 4.32$ fm^3/GeV. On the other hand, the background fluctuations from the participant model for other centralities are larger compared to the measured ones making the background-subtracted fluctuations negative. So it is not possible to obtain estimates of k_T for these centrality ranges based on the present model of participant fluctuations.

The measured multiplicity fluctuations can be viewed as combinations of correlated and uncorrelated fluctuations. If the particle production is completely uncorrelated, the system effectively behaves as an ideal gas, and the multiplicity distribution is expected to follow a Poisson distribution ($\omega_{\mathrm{ch}} = 1$). For central collisions, fluctuations above the Poisson estimation gives, $\omega_{\mathrm{ch}} = 1.15 \pm 0.06$, which in turn implies a value of $k_T = 27.9 \pm 3.18$ fm^3/GeV.

It may be noted that other sources likely also contribute to the background of the measured multiplicity fluctuations. A quantitative determination of these effects requires further studies and theoretical modeling, which is beyond the scope of this work. In view of this, the estimation of k_T from the background-subtracted event-by-event multiplicity fluctuation provides an upper limit of its value.

It is imperative to put the extracted values of k_T in perspective with respect to that of normal nuclear matter. The incompressibility constant of normal nuclear matter at pressure P, expressed as $K_0 = 9(\partial P/\partial \rho)$ at zero temperature and normal nuclear density, $\rho = \rho_0$, has been determined to be $K_0 = 240 \pm 20$ MeV [54–56]. Using the relation, $k_T = (9/\rho K_0)$, one obtains the isothermal compressibility of nuclear matter to be $k_T \simeq 234 \pm 20$ fm^3/GeV. This is consistent with the expectation that normal nuclear matter at low temperature is more compressible than the high temperature matter produced at LHC energies (as of Eq. 3). From the above estimation, the value of $k_T = 27.9 \pm 3.18$ fm^3/GeV, which corresponds to multiplicity fluctuations above the Poisson expectation, serves as a conservative upper limit, and is even significantly below the normal nuclear matter at low temperature.

6 Summary

Measurements of event-by-event fluctuations of charged-particle multiplicities are reported as a function of centrality in Pb–Pb collisions at $\sqrt{s_{\mathrm{NN}}} = 2.76$ TeV. The mean, standard deviation, and scaled variances of charged-particle multiplicities are presented for $|\eta| < 0.8$ and $0.2 < p_{\mathrm{T}} < 2.0$ GeV/c as a function of centrality. A monotonically decreasing trend for the scaled variance is observed from peripheral to central collisions. Corresponding results from HIJING and AMPT event generators show a mismatch with the experimental results. The scaled variance of the multiplicity decreases with the reduction of the η acceptance of the detector as well as with the decrease of the p_{T} range. The multiplicity fluctuations are compared to the results from lower beam energies as reported by the PHENIX experiment. For the same acceptance, the observed scaled variances at RHIC energies are smaller compared to those observed at the LHC.

As multiplicity fluctuations are related to the isothermal compressibility of the system, the measured fluctuations are used to estimate k_T in central Pb–Pb collisions at $\sqrt{s_{\mathrm{NN}}} = 2.76$ TeV. The multiplicity fluctuations above the Poisson expectation case yields $k_T = 27.9 \pm 3.18$ fm^3/GeV, which may still contain contributions from additional uncorrelated particle production as well as from several non-thermal sources as discussed in Sect. 5. Proper modeling of background subtraction needs to be developed by accounting for all possible contributions from different physics origins, which is beyond the scope of the present work. This result serves as a conservative upper limit of k_T until various contributions to the background are properly understood and evaluated. The estimation of k_T at lower collision energies and for different system-sizes is an interesting way to explore the QCD phase diagram from thermodynamics point of view.

Acknowledgements The ALICE Collaboration would like to thank all its engineers and technicians for their invaluable contributions to the construction of the experiment and the CERN accelerator teams for the outstanding performance of the LHC complex. The ALICE Collaboration gratefully acknowledges the resources and support provided by all Grid centres and the Worldwide LHC Computing Grid (WLCG) collaboration. The ALICE Collaboration acknowledges the following funding agencies for their support in building and running the ALICE detector: A. I. Alikhanyan National Science Laboratory (Yerevan Physics Institute) Foundation (ANSL), State Committee of Science and World Federation of Scientists (WFS), Armenia; Austrian Academy of Sciences, Austrian Science Fund (FWF): [M 2467-N36] and Nationalstiftung für Forschung, Technologie und Entwicklung, Austria; Ministry of Communications and High Technologies, National Nuclear Research Center, Azerbaijan; Conselho Nacional de Desenvolvimento Científico e Tecnológico (CNPq), Financiadora de Estudos e Projetos (Finep), Fundação de Amparo à Pesquisa do Estado de São Paulo (FAPESP) and Universidade Federal do Rio Grande do Sul (UFRGS), Brazil; Ministry of Education of China (MOEC) , Ministry of Science & Technology of China (MSTC) and National Natural Science Foundation of China (NSFC), China; Ministry of Science and Education and Croatian Science Foundation, Croatia; Centro de Aplicaciones Tecnológicas y Desarrollo Nuclear (CEADEN), Cubaenergía, Cuba; Ministry of Education, Youth and Sports of the Czech Republic, Czech Republic; The Danish Council for Independent Research | Natural Sciences, the VILLUM FONDEN and Danish National Research Foundation (DNRF), Denmark; Helsinki Institute of Physics (HIP), Finland; Commissariat à l'Energie Atomique (CEA) and Institut National de Physique Nucléaire et de Physique des Particules (IN2P3) and Centre National de la Recherche Scientifique (CNRS), France; Bundesministerium für Bildung und Forschung (BMBF) and GSI Helmholtzzentrum für Schwerionenforschung GmbH, Germany; General Secretariat for Research and Technology, Ministry of Education, Research and Religions, Greece; National Research, Development and Innovation Office, Hungary; Department of Atomic Energy Government of India (DAE), Department of Science and Technology, Government of India (DST), University Grants Commission, Government of India (UGC) and Council of Scientific and Industrial Research (CSIR), India; Indonesian Institute of Science, Indonesia; Istituto Nazionale di Fisica Nucleare (INFN), Italy; Institute for Innovative Science and Technology, Nagasaki Institute of Applied Science (IIST), Japanese Ministry of Education, Culture, Sports, Science and Technology (MEXT) and Japan Society for the Promotion of Science (JSPS) KAKENHI, Japan; Consejo Nacional de Ciencia (CONACYT) y Tecnología, through Fondo de Cooperación Internacional en Ciencia y Tecnología (FONCICYT) and Dirección General de Asuntos del Personal Academico (DGAPA), Mexico; Nederlandse Organisatie voor Wetenschappelijk Onderzoek (NWO), Netherlands; The Research Council of Norway, Norway; Commission on Science and Technology for Sustainable Development in the South (COMSATS), Pakistan; Pontificia Universidad Católica del Perú, Peru; Ministry of Education and Science, National Science Centre and WUT ID-UB, Poland; Korea Institute of Science and Technology Information and National Research Foundation of Korea (NRF), Republic of Korea; Ministry of Education and Scientific Research, Institute of Atomic Physics and Ministry of Research and Innovation and Institute of Atomic Physics, Romania; Joint Institute for Nuclear Research (JINR), Ministry of Education and Science of the Russian Federation, National Research Centre Kurchatov Institute, Russian Science Foundation and Russian Foundation for Basic Research, Russia; Ministry of Education, Science, Research and Sport of the Slovak Republic, Slovakia; National Research Foundation of South Africa, South Africa; Swedish Research Council (VR) and Knut & Alice Wallenberg Foundation (KAW), Sweden; European Organization for Nuclear Research, Switzerland; Suranaree University of Technology (SUT), National Science and Technology Development Agency (NSDTA) and Office of the Higher Education Commission under NRU project of Thailand, Thailand; Turkish Energy, Nuclear and Mineral Research Agency (TENMAK), Turkey; National Academy of Sciences of Ukraine, Ukraine; Science and Technology Facilities Council (STFC), United Kingdom; National Science Foundation of the United States of America (NSF) and United States Department of Energy, Office of Nuclear Physics (DOE NP), United States of America.

Data Availability Statement This manuscript has no associated data or the data will not be deposited. [Authors' comment: Manuscript has associated data in a HEPData repository at https://www.hepdata.net/.]

Funded by SCOAP^3.

References

1. H. Satz, The quark–gluon plasma: a short introduction. Nucl. Phys. A **862–863**, 4–12 (2011). https://doi.org/10.1016/j.nuclphysa.2011.05.014. arXiv:1101.3937 [hep-ph]
2. C. Ratti, M.A. Thaler, W. Weise, Phases of QCD: lattice thermodynamics and a field theoretical model. Phys. Rev. D **73**, 014019 (2006). https://doi.org/10.1103/PhysRevD.73.014019. arXiv:hep-ph/0506234
3. S.A. Bass, M. Gyulassy, H. Stoecker, W. Greiner, Signatures of quark gluon plasma formation in high-energy heavy ion collisions: a critical review. J. Phys. G **25**, R1–R57 (1999). https://doi.org/10.1088/0954-3899/25/3/013. arXiv:hep-ph/9810281
4. P. Braun-Munzinger, V. Koch, T. Schäfer, J. Stachel, Properties of hot and dense matter from relativistic heavy ion collisions. Phys. Rep. **621**, 76–126 (2016). https://doi.org/10.1016/j.physrep.2015.12.003. arXiv:1510.00442 [nucl-th]
5. A. Andronic, P. Braun-Munzinger, K. Redlich, J. Stachel, Decoding the phase structure of QCD via particle production at high energy. Nature **561**(7723), 321–330 (2018). https://doi.org/10.1038/s41586-018-0491-6. arXiv:1710.09425 [nucl-th]
6. M.A. Stephanov, K. Rajagopal, E.V. Shuryak, Signatures of the tricritical point in QCD. Phys. Rev. Lett. **81**, 4816–4819 (1998). https://doi.org/10.1103/PhysRevLett.81.4816. arXiv:hep-ph/9806219
7. M.A. Stephanov, K. Rajagopal, E.V. Shuryak, Event-by-event fluctuations in heavy ion collisions and the QCD critical point. Phys. Rev. D **60**, 114028 (1999). https://doi.org/10.1103/PhysRevD.60.114028. arXiv:hep-ph/9903292
8. V. Koch, M. Bleicher, S. Jeon, Event-by-event fluctuations and the QGP. Nucl. Phys. A **698**, 261–268 (2002). https://doi.org/10.1016/S0375-9474(02)00716-9. arXiv:nucl-th/0103084
9. S. Jeon, V. Koch, Charged particle ratio fluctuation as a signal for QGP. Phys. Rev. Lett. **85**, 2076–2079 (2000). https://doi.org/10.1103/PhysRevLett.85.2076. arXiv:hep-ph/0003168
10. S. Jeon, V. Koch, in Quark-Gluon Plasma 3, edited by R. C. Hwa and X. N. Wang (World Scientific, Singapore, 2004), p. 430-490. https://doi.org/10.1142/9789812795533_0007. arXiv:hep-ph/0304012 [hep-ph]
11. F. Karsch, S. Ejiri, K. Redlich, Hadronic fluctuations in the QGP. Nucl. Phys. A **774**, 619–622 (2006). https://doi.org/10.1016/j.nuclphysa.2006.06.099. arXiv:hep-ph/0510126
12. B. Stokic, B. Friman, K. Redlich, Kurtosis and compressibility near the chiral phase transition. Phys. Lett. B **673**, 192–196 (2009). https://doi.org/10.1016/j.physletb.2009.02.018. arXiv:0809.3129 [hep-ph]
13. L. Van Hove, Two problems concerning hot hadronic matter and high-energy collisions (equilibrium formation, plasma deflagration). Z. Phys. C **21**(1), 93–98 (1983)
14. A. Bialas, Charge fluctuations in a quark anti-quark system. Phys. Lett. B **532**, 249–251 (2002). https://doi.org/10.1016/S0370-2693(02)01550-2. arXiv:hep-ph/0203047
15. G. Baym, H. Heiselberg, Event-by-event fluctuations in ultrarelativistic heavy ion collisions. Phys. Lett. B **469**, 7–11 (1999). https://doi.org/10.1016/S0370-2693(99)01263-0. arXiv:nucl-th/9905022
16. E.V. Shuryak, Event per event analysis of heavy ion collisions and thermodynamical fluctuations. Phys. Lett. B **423**, 9–14 (1998). https://doi.org/10.1016/S0370-2693(98)00127-0. arXiv:hep-ph/9704456

17. S. Mrowczynski, Hadronic matter compressibility from event by event analysis of heavy ion collisions. Phys. Lett. B **430**, 9–14 (1998). https://doi.org/10.1016/S0370-2693(98)00492-4. arXiv:nucl-th/9712030
18. M. Gazdzicki, M.I. Gorenstein, S. Mrowczynski, Fluctuations and deconfinement phase transition in nucleus nucleus collisions. Phys. Lett. B **585**, 115–121 (2004). https://doi.org/10.1016/j.physletb.2004.01.077. arXiv:hep-ph/0304052
19. M. Mukherjee, S. Basu, S. Choudhury, T.K. Nayak, Fluctuations in charged particle multiplicities in relativistic heavy-ion collisions. J. Phys. G **43**(8), 085102 (2016). https://doi.org/10.1088/0954-3899/43/8/085102. arXiv:1603.02083 [nucl-ex]
20. M. Mukherjee, S. Basu, A. Chatterjee, S. Chatterjee, S.P. Adhya, S. Thakur, T.K. Nayak, Isothermal compressibility of hadronic matter formed in relativistic nuclear collisions. Phys. Lett. B **784**, 1–5 (2018). https://doi.org/10.1016/j.physletb.2018.07.021. arXiv:1708.08692 [nucl-ex]
21. S. Basu, S. Chatterjee, R. Chatterjee, T.K. Nayak, B.K. Nandi, Specific heat of matter formed in relativistic nuclear collisions. Phys. Rev. C **94**(4), 044901 (2016). https://doi.org/10.1103/PhysRevC.94.044901. arXiv:1601.05631 [nucl-ex]
22. H. Heiselberg, Event-by-event physics in relativistic heavy ion collisions. Phys. Rep. **351**, 161–194 (2001). https://doi.org/10.1016/S0370-1573(00)00140-X. arXiv:nucl-th/0003046
23. V.V. Begun, M. Gazdzicki, M.I. Gorenstein, O.S. Zozulya, Particle number fluctuations in canonical ensemble. Phys. Rev. C **70**, 034901 (2004). https://doi.org/10.1103/PhysRevC.70.034901. arXiv:nucl-th/0404056
24. S. Basu, S. Thakur, T.K. Nayak, C.A. Pruneau, Multiplicity and pseudorapidity density distributions of charged particles produced in pp, pA and AA collisions at RHIC & LHC energies. J. Phys. G **48**(2), 025103 (2020). https://doi.org/10.1088/1361-6471/abc05c. arXiv:2008.07802 [nucl-ex]
25. E-802 Collaboration, T. Abbott et al., Multiplicity distributions from central collisions of O-16 + Cu at 14.6/A-GeV/c and intermittency. Phys. Rev. C **52**, 2663–2678 (1995). https://doi.org/10.1103/PhysRevC.52.2663
26. WA98 Collaboration, M.M. Aggarwal et al., Event-by-event fluctuations in particle multiplicities and transverse energy produced in 158-A-GeV Pb + Pb collisions. Phys. Rev. C **65**, 054912 (2002). https://doi.org/10.1103/PhysRevC.65.054912. arXiv:nucl-ex/0108029
27. NA49 Collaboration, C. Alt et al., Centrality and system size dependence of multiplicity fluctuations in nuclear collisions at 158-A/GeV. Phys. Rev. C **75**, 064904 (2007). https://doi.org/10.1103/PhysRevC.75.064904. arXiv:nucl-ex/0612010
28. NA49 Collaboration, C. Alt et al., Electric charge fluctuations in central Pb + Pb collisions at 20-A-GeV, 30-A-GeV, 40-A-GeV, 80-A-GeV, and 158-A-GeV. Phys. Rev. C **70**, 064903 (2004). https://doi.org/10.1103/PhysRevC.70.064903. arXiv:nucl-ex/0406013
29. CERES/NA45 Collaboration, H. Sako, H. Appelshaeuser, Event-by-event fluctuations at 40-A-GeV/c, 80-A-GeV/c, and 158-A-GeV/c in Pb + Au collisions. J. Phys. G **30**, S1371–S1376 (2004). https://doi.org/10.1088/0954-3899/30/8/130. arXiv:nucl-ex/0403037
30. PHOBOS Collaboration, K. Wozniak et al., Charged particle multiplicity fluctuations in Au + Au collisions at s(NN)**(1/2) = 200-GeV. J. Phys. G **30**, S1377–S1380 (2004). https://doi.org/10.1088/0954-3899/30/8/131
31. PHENIX Collaboration, A. Adare et al., Charged hadron multiplicity fluctuations in Au + Au and Cu + Cu collisions from $\sqrt{s_{NN}}$ = 22.5 to 200 GeV. Phys. Rev. C **78**, 044902 (2008). https://doi.org/10.1103/PhysRevC.78.044902. arXiv:0805.1521 [nucl-ex]
32. D. Sahu, S. Tripathy, R. Sahoo, A.R. Dash, Multiplicity dependence of shear viscosity, isothermal compressibility and speed of sound in *pp* collisions at $\sqrt{s}$ = 7 TeV. Eur. Phys. J. A **56**(7), 187 (2020). https://doi.org/10.1140/epja/s10050-020-00197-7. arXiv:2002.05054 [hep-ph]
33. V. Begun, M. Mackowiak-Pawlowska, Multi moment cancellation of participant fluctuations—MMCP method. arXiv:1705.01110 [nucl-th]
34. P. Braun-Munzinger, A. Rustamov, J. Stachel, Bridging the gap between event-by-event fluctuation measurements and theory predictions in relativistic nuclear collisions. Nucl. Phys. A **960**, 114–130 (2017). https://doi.org/10.1016/j.nuclphysa.2017.01.011. arXiv:1612.00702 [nucl-th]
35. N. Sharma, J. Cleymans, B. Hippolyte, M. Paradza, A comparison of p–p, p–Pb, Pb–Pb collisions in the thermal model: multiplicity dependence of thermal parameters. Phys. Rev. C **99**(4), 044914 (2019). https://doi.org/10.1103/PhysRevC.99.044914. arXiv:1811.00399 [hep-ph]
36. ALICE Collaboration, J. Adam et al., Production of light nuclei and anti-nuclei in pp and Pb–Pb collisions at energies available at the CERN Large Hadron Collider. Phys. Rev. C **93**(2), 024917 (2016). https://doi.org/10.1103/PhysRevC.93.024917. arXiv:1506.08951 [nucl-ex]
37. S. Mrowczynski, Overview of event-by-event fluctuations. Acta Phys. Polon. B **40**, 1053–1074 (2009). arXiv:0902.0825 [nucl-th]
38. ALICE Collaboration, K. Aamodt et al., The ALICE experiment at the CERN LHC. JINST **3**, S08002 (2008). https://doi.org/10.1088/1748-0221/3/08/S08002
39. ALICE Collaboration, B. Abelev et al., Centrality determination of Pb–Pb collisions at $\sqrt{s_{NN}}$ = 2.76 TeV with ALICE. Phys. Rev. C **88**(4), 044909 (2013). https://doi.org/10.1103/PhysRevC.88.044909. arXiv:1301.4361 [nucl-ex]
40. R. Brun, F. Bruyant, F. Carminati, S. Giani, M. Maire, A. McPherson, G. Patrick, L. Urban, GEANT detector description and simulation tool, Tech. rep., CERN (1994). https://doi.org/10.17181/CERN.MUHF.DMJ1
41. M.L. Miller, K. Reygers, S.J. Sanders, P. Steinberg, Glauber modeling in high energy nuclear collisions. Annu. Rev. Nucl. Part. Sci. **57**, 205–243 (2007). https://doi.org/10.1146/annurev.nucl.57.090506.123020. arXiv:nucl-ex/0701025
42. X. Luo, J. Xu, B. Mohanty, N. Xu, Volume fluctuation and auto-correlation effects in the moment analysis of net-proton multiplicity distributions in heavy-ion collisions. J. Phys. G **40**, 105104 (2013). https://doi.org/10.1088/0954-3899/40/10/105104. arXiv:1302.2332 [nucl-ex]
43. N.R. Sahoo, S. De, T.K. Nayak, Baseline study for higher moments of net-charge distributions at energies available at the BNL Relativistic Heavy Ion Collider. Phys. Rev. C **87**(4), 044906 (2013). https://doi.org/10.1103/PhysRevC.87.044906. arXiv:1210.7206 [nucl-ex]
44. A. Bzdak, V. Koch, Local efficiency corrections to higher order cumulants. Phys. Rev. C **91**(2), 027901 (2015). https://doi.org/10.1103/PhysRevC.91.027901. arXiv:1312.4574 [nucl-th]
45. X. Luo, Unified description of efficiency correction and error estimation for moments of conserved quantities in heavy-ion collisions. Phys. Rev. C **91**(3), 034907 (2015). https://doi.org/10.1103/PhysRevC.94.059901. arXiv:1410.3914 [physics.data-an] [Erratum: Phys. Rev. C **94**, 059901 (2016)]
46. W.-T. Deng, X.-N. Wang, R. Xu, Gluon shadowing and hadron production in heavy-ion collisions at LHC. Phys. Lett. B **701**, 133–136 (2011). https://doi.org/10.1016/j.physletb.2011.05.040. arXiv:1011.5907 [nucl-th]
47. X. Luo, Error estimation for moments analysis in heavy ion collision experiment. J. Phys. G **39**, 025008 (2012). https://doi.org/10.1088/0954-3899/39/2/025008. arXiv:1109.0593 [physics.data-an]

48. Z.-W. Lin, C.M. Ko, B.-A. Li, B. Zhang, S. Pal, A multi-phase transport model for relativistic heavy ion collisions. Phys. Rev. C **72**, 064901 (2005). https://doi.org/10.1103/PhysRevC.72.064901. arXiv:nucl-th/0411110
49. PHENIX Collaboration, J.T. Mitchell, Scaling properties of fluctuation and correlation results from PHENIX. J. Phys. G **34**, S911–914 (2007). https://doi.org/10.1088/0954-3899/34/8/S124. arXiv:nucl-ex/0701062
50. ALICE Collaboration, S. Acharya et al., Transverse momentum spectra and nuclear modification factors of charged particles in pp, p-Pb and Pb–Pb collisions at the LHC. JHEP **11**, 013 (2018). https://doi.org/10.1007/JHEP11(2018)013. arXiv:1802.09145 [nucl-ex]
51. ALICE Collaboration, B. Abelev et al., Centrality dependence of π, K, p production in Pb–Pb collisions at $\sqrt{s_{NN}} = 2.76$ TeV. Phys. Rev. C **88**, 044910 (2013). https://doi.org/10.1103/PhysRevC.88.044910. arXiv:1303.0737 [hep-ex]
52. ALICE Collaboration, S. Acharya et al., Production of ^{4}He and $^4\overline{\text{He}}$ in Pb–Pb collisions at $\sqrt{s_{\text{NN}}} = 2.76$ TeV at the LHC. Nucl. Phys. A **971**, 1–20 (2018). https://doi.org/10.1016/j.nuclphysa.2017.12.004. arXiv:1710.07531 [nucl-ex]
53. M. Petrán, J. Letessier, V. Petráček, J. Rafelski, Hadron production and quark-gluon plasma hadronization in Pb–Pb collisions at $\sqrt{s_{NN}} = 2.76$ TeV. Phys. Rev. C **88**(3), 034907 (2013). https://doi.org/10.1103/PhysRevC.88.034907. arXiv:1303.2098 [hep-ph]
54. J.P. Blaizot, Nuclear compressibilities. Phys. Rep. **64**, 171–248 (1980). https://doi.org/10.1016/0370-1573(80)90001-0
55. P. Danielewicz, R. Lacey, W.G. Lynch, Determination of the equation of state of dense matter. Science **298**, 1592–1596 (2002). https://doi.org/10.1126/science.1078070. arXiv:nucl-th/0208016
56. J.R. Stone, N.J. Stone, S.A. Moszkowski, Incompressibility in finite nuclei and nuclear matter. Phys. Rev. C **89**(4), 044316 (2014). https://doi.org/10.1103/PhysRevC.89.044316. arXiv:1404.0744 [nucl-th]

ALICE Collaboration

S. Acharya[143], D. Adamová[98], A. Adler[76], J. Adolfsson[83], G. Aglieri Rinella[35], M. Agnello[31], N. Agrawal[55], Z. Ahammed[143], S. Ahmad[16], S. U. Ahn[78], I. Ahuja[39], Z. Akbar[52], A. Akindinov[95], M. Al-Turany[110], S. N. Alam[41], D. Aleksandrov[91], B. Alessandro[61], H. M. Alfanda[7], R. Alfaro Molina[73], B. Ali[16], Y. Ali[14], A. Alici[26], N. Alizadehvandchali[127], A. Alkin[35], J. Alme[21], T. Alt[70], L. Altenkamper[21], I. Altsybeev[115], M. N. Anaam[7], C. Andrei[49], D. Andreou[93], A. Andronic[146], M. Angeletti[35], V. Anguelov[107], F. Antinori[58], P. Antonioli[55], C. Anuj[16], N. Apadula[82], L. Aphecetche[117], H. Appelshäuser[70], S. Arcelli[26], R. Arnaldi[61], I. C. Arsene[20], M. Arslandok[107,148], A. Augustinus[35], R. Averbeck[110], S. Aziz[80], M. D. Azmi[16], A. Badalà[57], Y. W. Baek[42], X. Bai[110,131], R. Bailhache[70], Y. Bailung[51], R. Bala[104], A. Balbino[31], A. Baldisseri[140], B. Balis[2], M. Ball[44], D. Banerjee[4], R. Barbera[27], L. Barioglio[25,108], M. Barlou[87], G. G. Barnaföldi[147], L. S. Barnby[97], V. Barret[137], C. Bartels[130], K. Barth[35], E. Bartsch[70], F. Baruffaldi[28], N. Bastid[137], S. Basu[83], G. Batigne[117], B. Batyunya[77], D. Bauri[50], J. L. Bazo Alba[114], I. G. Bearden[92], C. Beattie[148], I. Belikov[139], A. D. C. Bell Hechavarria[146], F. Bellini[26,35], R. Bellwied[127], S. Belokurova[115], V. Belyaev[96], G. Bencedi[71], S. Beole[25], A. Bercuci[49], Y. Berdnikov[101], A. Berdnikova[107], D. Berenyi[147], L. Bergmann[107], M. G. Besoiu[69], L. Betev[35], P. P. Bhaduri[143], A. Bhasin[104], I. R. Bhat[104], M. A. Bhat[4], B. Bhattacharjee[43], P. Bhattacharya[23], L. Bianchi[25], N. Bianchi[53], J. Bielčík[38], J. Bielčíková[98], J. Biernat[120], A. Bilandzic[108], G. Biro[147], S. Biswas[4], J. T. Blair[121], D. Blau[91], M. B. Blidaru[110], C. Blume[70], G. Boca[29,59], F. Bock[99], A. Bogdanov[96], S. Boi[23], J. Bok[63], L. Boldizsár[147], A. Bolozdynya[96], M. Bombara[39], P. M. Bond[35], G. Bonomi[59,142], H. Borel[140], A. Borissov[84], H. Bossi[148], E. Botta[25], L. Bratrud[70], P. Braun-Munzinger[110], M. Bregant[123], M. Broz[38], G. E. Bruno[34,109], M. D. Buckland[130], D. Budnikov[111], H. Buesching[70], S. Bufalino[31], O. Bugnon[117], P. Buhler[116], Z. Buthelezi[74,134], J. B. Butt[14], S. A. Bysiak[120], D. Caffarri[93], M. Cai[7,28], H. Caines[148], A. Caliva[110], E. Calvo Villar[114], J. M. M. Camacho[122], R. S. Camacho[46], P. Camerini[24], F. D. M. Canedo[123], F. Carnesecchi[26,35], R. Caron[140], J. Castillo Castellanos[140], E. A. R. Casula[23], F. Catalano[31], C. Ceballos Sanchez[77], P. Chakraborty[50], S. Chandra[143], S. Chapeland[35], M. Chartier[130], S. Chattopadhyay[143], S. Chattopadhyay[112], A. Chauvin[23], T. G. Chavez[46], C. Cheshkov[138], B. Cheynis[138], V. Chibante Barroso[35], D. D. Chinellato[124], S. Cho[63], P. Chochula[35], P. Christakoglou[93], C. H. Christensen[92], P. Christiansen[83], T. Chujo[136], C. Cicalo[56], L. Cifarelli[26], F. Cindolo[55], M. R. Ciupek[110], G. Clai[55,a], J. Cleymans[126,e], F. Colamaria[54], J. S. Colburn[113], D. Colella[34,54,109,147], A. Collu[82], M. Colocci[26,35], M. Concas[61,b], G. Conesa Balbastre[81], Z. Conesa del Valle[80], G. Contin[24], J. G. Contreras[38], M. L. Coquet[140], T. M. Cormier[99], P. Cortese[32], M. R. Cosentino[125], F. Costa[35], S. Costanza[29,59], P. Crochet[137], R. Cruz-Torres[82], E. Cuautle[71], P. Cui[7], L. Cunqueiro[99], A. Dainese[58], F. P. A. Damas[117,140], M. C. Danisch[107], A. Danu[69], I. Das[112], P. Das[89], P. Das[4], S. Das[4], S. Dash[50], S. De[89], A. De Caro[30], G. de Cataldo[54], L. De Cilladi[25], J. de Cuveland[40], A. De Falco[23], D. De Gruttola[30], N. De Marco[61], C. De Martin[24], S. De Pasquale[30], S. Deb[51], H. F. Degenhardt[123], K. R. Deja[144], L. Dello Stritto[30], S. Delsanto[25], W. Deng[7], P. Dhankher[19], D. Di Bari[34], A. Di Mauro[35], R. A. Diaz[8], T. Dietel[126], Y. Ding[138,7], R. Divià[35], D. U. Dixit[19], Ø. Djuvsland[21], U. Dmitrieva[65], J. Do[63], A. Dobrin[69], B. Dönigus[70], O. Dordic[20], A. K. Dubey[143], A. Dubla[93,110], S. Dudi[103], M. Dukhishyam[89], P. Dupieux[137], N. Dzalaiova[13], T. M. Eder[146], R. J. Ehlers[99], V. N. Eikeland[21], F. Eisenhut[70], D. Elia[54], B. Erazmus[117], F. Ercolessi[26], F. Erhardt[102], A. Erokhin[115], M. R. Ersdal[21], B. Espagnon[80], G. Eulisse[35], D. Evans[113], S. Evdokimov[94], L. Fabbietti[108], M. Faggin[28], J. Faivre[81], F. Fan[7], A. Fantoni[53], M. Fasel[99], P. Fecchio[31], A. Feliciello[61], G. Feofilov[115], A. Fernández Téllez[46], A. Ferrero[140], A. Ferretti[25], V. J. G. Feuillard[107], J. Figiel[120], S. Filchagin[111], D. Finogeev[65], F. M. Fionda[21,56], G. Fiorenza[35,109], F. Flor[127], A. N. Flores[121], S. Foertsch[74], P. Foka[110], S. Fokin[91], E. Fragiacomo[62], E. Frajna[147], U. Fuchs[35], N. Funicello[30], C. Furget[81], A. Furs[65], J. J. Gaardhøje[92], M. Gagliardi[25], A. M. Gago[114], A. Gal[139], C. D. Galvan[122], P. Ganoti[87], C. Garabatos[110], J. R. A. Garcia[46], E. Garcia-Solis[10], K. Garg[117], C. Gargiulo[35], A. Garibli[90], K. Garner[146], P. Gasik[110], E. F. Gauger[121], A. Gautam[129], M. B. Gay Ducati[72], M. Germain[117], J. Ghosh[112], P. Ghosh[143], S. K. Ghosh[4], M. Giacalone[26], P. Gianotti[53], P. Giubellino[61,110], P. Giubilato[28], A. M. C. Glaenzer[140], P. Glässel[107], D. J. Q. Goh[85], V. Gonzalez[145], L. H. González-Trueba[73], S. Gorbunov[40], M. Gorgon[2], L. Görlich[120], S. Gotovac[36], V. Grabski[73], L. K. Graczykowski[144], L. Greiner[82], A. Grelli[64], C. Grigoras[35], V. Grigoriev[96], A. Grigoryan[1,e], S. Grigoryan[77,1], O. S. Groettvik[21], F. Grosa[35,61], J. F. Grosse-Oetringhaus[35], R. Grosso[110], G. G. Guardiano[124], R. Guernane[81], M. Guilbaud[117], K. Gulbrandsen[92], T. Gunji[135], A. Gupta[104], R. Gupta[104], I. B. Guzman[46], S. P. Guzman[46], L. Gyulai[147], M. K. Habib[110], C. Hadjidakis[80], G. Halimoglu[70], H. Hamagaki[85], G. Hamar[147], M. Hamid[7], R. Hannigan[121], M. R. Haque[89,144], A. Harlenderova[110], J. W. Harris[148], A. Harton[10], J. A. Hasenbichler[35], H. Hassan[99], D. Hatzifotiadou[55], P. Hauer[44], L. B. Havener[148], S. Hayashi[135], S. T. Heckel[108], E. Hellbär[70], H. Helstrup[37], T. Herman[38], E. G. Hernandez[46], G. Herrera Corral[9], F. Herrmann[146], K. F. Hetland[37], H. Hillemanns[35], C. Hills[130], B. Hippolyte[139], B. Hofman[64], B. Hohlweger[93,108], J. Honermann[146], G. H. Hong[149], D. Horak[38], S. Hornung[110], A. Horzyk[2], R. Hosokawa[15], P. Hristov[35], C. Huang[80], C. Hughes[133], P. Huhn[70], T. J. Humanic[100], H. Hushnud[112], L. A. Husova[146], A. Hutson[127], D. Hutter[40],

J. P. Iddon[35,130], R. Ilkaev[111], H. Ilyas[14], M. Inaba[136], G. M. Innocenti[35], M. Ippolitov[91], A. Isakov[38,98], M. S. Islam[112], M. Ivanov[110], V. Ivanov[101], V. Izucheev[94], M. Jablonski[2], B. Jacak[82], N. Jacazio[35], P. M. Jacobs[82], S. Jadlovska[119], J. Jadlovsky[119], S. Jaelani[64], C. Jahnke[123,124], M. J. Jakubowska[144], M. A. Janik[144], T. Janson[76], M. Jercic[102], O. Jevons[113], F. Jonas[99,146], P. G. Jones[113], J. M. Jowett [35,110], J. Jung[70], M. Jung[70], A. Junique[35], A. Jusko[113], J. Kaewjai[118], P. Kalinak[66], A. Kalweit[35], V. Kaplin[96], S. Kar[7], A. Karasu Uysal[79], D. Karatovic[102], O. Karavichev[65], T. Karavicheva[65], P. Karczmarczyk[144], E. Karpechev[65], A. Kazantsev[91], U. Kebschull[76], R. Keidel[48], D. L. D. Keijdener[64], M. Keil[35], B. Ketzer[44], Z. Khabanova[93], A. M. Khan[7], S. Khan[16], A. Khanzadeev[101], Y. Kharlov[94], A. Khatun[16], A. Khuntia[120], B. Kileng[37], B. Kim[17,63], D. Kim[149], D. J. Kim[128], E. J. Kim[75], J. Kim[149], J. S. Kim[42], J. Kim[107], J. Kim[149], J. Kim[75], M. Kim[107], S. Kim[18], T. Kim[149], S. Kirsch[70], I. Kisel[40], S. Kiselev[95], A. Kisiel[144], J. P. Kitowski[2], J. L. Klay[6], J. Klein[35], S. Klein[82], C. Klein-Bösing[146], M. Kleiner[70], T. Klemenz[108], A. Kluge[35], A. G. Knospe[127], C. Kobdaj[118], M. K. Köhler[107], T. Kollegger[110], A. Kondratyev[77], N. Kondratyeva[96], E. Kondratyuk[94], J. Konig[70], S. A. Konigstorfer[108], P. J. Konopka[2,35], G. Kornakov[144], S. D. Koryciak[2], L. Koska[119], A. Kotliarov[98], O. Kovalenko[88], V. Kovalenko[115], M. Kowalski[120], I. Králik[66], A. Kravčáková[39], L. Kreis[110], M. Krivda[66,113], F. Krizek[98], K. Krizkova Gajdosova[38], M. Kroesen[107], M. Krüger[70], E. Kryshen[101], M. Krzewicki[40], V. Kučera[35], C. Kuhn[139], P. G. Kuijer[93], T. Kumaoka[136], D. Kumar[143], L. Kumar[103], N. Kumar[103], S. Kundu[35,89], P. Kurashvili[88], A. Kurepin[65], A. B. Kurepin[65], A. Kuryakin[111], S. Kushpil[98], J. Kvapil[113], M. J. Kweon[63], J. Y. Kwon[63], Y. Kwon[149], S. L. La Pointe[40], P. La Rocca[27], Y. S. Lai[82], A. Lakrathok[118], M. Lamanna[35], R. Langoy[132], K. Lapidus[35], P. Larionov[53], E. Laudi[35], L. Lautner[35,108], R. Lavicka[38], T. Lazareva[115], R. Lea[24,59,142], J. Lee[136], J. Lehrbach[40], R. C. Lemmon[97], I. León Monzón[122], E. D. Lesser[19], M. Lettrich[35,108], P. Lévai[147], X. Li[11], X. L. Li[7], J. Lien[132], R. Lietava[113], B. Lim[17], S. H. Lim[17], V. Lindenstruth[40], A. Lindner[49], C. Lippmann[110], A. Liu[19], J. Liu[130], I. M. Lofnes[21], V. Loginov[96], C. Loizides[99], P. Loncar[36], J. A. Lopez[107], X. Lopez[137], E. López Torres[8], J. R. Luhder[146], M. Lunardon[28], G. Luparello[62], Y. G. Ma[41], A. Maevskaya[65], M. Mager[35], T. Mahmoud[44], A. Maire[139], M. Malaev[101], Q. W. Malik[20], L. Malinina[77,c], D. Mal'Kevich[95], N. Mallick[51], P. Malzacher[110], G. Mandaglio[33,57], V. Manko[91], F. Manso[137], V. Manzari[54], Y. Mao[7], J. Mareš[68], G. V. Margagliotti[24], A. Margotti[55], A. Marín[110], C. Markert[121], M. Marquard[70], N. A. Martin[107], P. Martinengo[35], J. L. Martinez[127], M. I. Martínez[46], G. Martínez García[117], S. Masciocchi[110], M. Masera[25], A. Masoni[56], L. Massacrier[80], A. Mastroserio[54,141], A. M. Mathis[108], O. Matonoha[83], P. F. T. Matuoka[123], A. Matyja[120], C. Mayer[120], A. L. Mazuecos[35], F. Mazzaschi[25], M. Mazzilli[35], M. A. Mazzoni[60,e], J. E. Mdhluli[134], A. F. Mechler[70], F. Meddi[22], Y. Melikyan[65], A. Menchaca-Rocha[73], E. Meninno[30,116], A. S. Menon[127], M. Meres[13], S. Mhlanga[74,126], Y. Miake[136], L. Micheletti[25,61], L. C. Migliorin[138], D. L. Mihaylov[108], K. Mikhaylov[77,95], A. N. Mishra[147], D. Miśkowiec[110], A. Modak[4], A. P. Mohanty[64], B. Mohanty[89], M. Mohisin Khan[16], Z. Moravcova[92], C. Mordasini[108], D. A. Moreira De Godoy[146], L. A. P. Moreno[46], I. Morozov[65], A. Morsch[35], T. Mrnjavac[35], V. Muccifora[53], E. Mudnic[36], D. Mühlheim[146], S. Muhuri[143], M. Mukherjee[4], J. D. Mulligan[82], A. Mulliri[23], M. G. Munhoz[123], R. H. Munzer[70], H. Murakami[135], S. Murray[126], L. Musa[35], J. Musinsky[66], C. J. Myers[127], J. W. Myrcha[144], B. Naik[50,134], R. Nair[88], B. K. Nandi[50], R. Nania[55], E. Nappi[54], M. U. Naru[14], A. F. Nassirpour[83], A. Nath[107], C. Nattrass[133], T. K. Nayak[89], A. Neagu[20], L. Nellen[71], S. V. Nesbo[37], G. Neskovic[40], D. Nesterov[115], B. S. Nielsen[92], S. Nikolaev[91], S. Nikulin[91], V. Nikulin[101], F. Noferini[55], S. Noh[12], P. Nomokonov[77], J. Norman[130], N. Novitzky[136], P. Nowakowski[144], A. Nyanin[91], J. Nystrand[21], M. Ogino[85], A. Ohlson[83], V. A. Okorokov[96], J. Oleniacz[144], A. C. Oliveira Da Silva[133], M. H. Oliver[148], A. Onnerstad[128], C. Oppedisano[61], A. Ortiz Velasquez[71], T. Osako[47], A. Oskarsson[83], J. Otwinowski[120], K. Oyama[85], Y. Pachmayer[107], S. Padhan[50], D. Pagano[59,142], G. Paić[71], A. Palasciano[54], J. Pan[145], S. Panebianco[140], P. Pareek[143], J. Park[63], J. E. Parkkila[128], S. P. Pathak[127], R. N. Patra[35,104], B. Paul[23], J. Pazzini[59,142], H. Pei[7], T. Peitzmann[64], X. Peng[7], L. G. Pereira[72], H. Pereira Da Costa[140], D. Peresunko[91], G. M. Perez[8], S. Perrin[140], Y. Pestov[5], V. Petráček[38], M. Petrovici[49], R. P. Pezzi[72,117], S. Piano[62], M. Pikna[13], P. Pillot[117], O. Pinazza[35,55], L. Pinsky[127], C. Pinto[27], S. Pisano[53], M. Płoskoń[82], M. Planinic[102], F. Pliquett[70], M. G. Poghosyan[99], B. Polichtchouk[94], S. Politano[31], N. Poljak[102], A. Pop[49], S. Porteboeuf-Houssais[137], J. Porter[82], V. Pozdniakov[77], S. K. Prasad[4], R. Preghenella[55], F. Prino[61], C. A. Pruneau[145], I. Pshenichnov[65], M. Puccio[35], S. Qiu[93], L. Quaglia[25], R. E. Quishpe[127], S. Ragoni[113], A. Rakotozafindrabe[140], L. Ramello[32], F. Rami[139], S. A. R. Ramirez[46], A. G. T. Ramos[34], T. A. Rancien[81], R. Raniwala[105], S. Raniwala[105], S. S. Räsänen[45], R. Rath[51], I. Ravasenga[93], K. F. Read[99,133], A. R. Redelbach[40], K. Redlich[88,d], A. Rehman[21], P. Reichelt[70], F. Reidt[35], H. A. Reme-ness[37], R. Renfordt[70], Z. Rescakova[39], K. Reygers[107], A. Riabov[101], V. Riabov[101], T. Richert[83,92], M. Richter[20], W. Riegler[35], F. Riggi[27], C. Ristea[69], S. P. Rode[51], M. Rodríguez Cahuantzi[46], K. Røed[20], R. Rogalev[94], E. Rogochaya[77], T. S. Rogoschinski[70], D. Rohr[35], D. Röhrich[21], P. F. Rojas[46], P. S. Rokita[144], F. Ronchetti[53], A. Rosano[33,57], E. D. Rosas[71], A. Rossi[58], A. Rotondi[29,59], A. Roy[51], P. Roy[112], S. Roy[50], N. Rubini[26], O. V. Rueda[83], R. Rui[24], B. Rumyantsev[77], P. G. Russek[2], A. Rustamov[90], E. Ryabinkin[91], Y. Ryabov[101], A. Rybicki[120], H. Rytkonen[128], W. Rzesa[144], O. A. M. Saarimaki[45], R. Sadek[117], S. Sadovsky[94], J. Saetre[21], K. Šafařík[38], S. K. Saha[143], S. Saha[89], B. Sahoo[50], P. Sahoo[50], R. Sahoo[51],

S. Sahoo[67], D. Sahu[51], P. K. Sahu[67], J. Saini[143], S. Sakai[136], S. Sambyal[104], V. Samsonov[96,101,e], D. Sarkar[145], N. Sarkar[143], P. Sarma[43], V. M. Sarti[108], M. H. P. Sas[148], J. Schambach[99,121], H. S. Scheid[70], C. Schiaua[49], R. Schicker[107], A. Schmah[107], C. Schmidt[110], H. R. Schmidt[106], M. O. Schmidt[107], M. Schmidt[106], N. V. Schmidt[70,99], A. R. Schmier[133], R. Schotter[139], J. Schukraft[35], Y. Schutz[139], K. Schwarz[110], K. Schweda[110], G. Scioli[26], E. Scomparin[61], J. E. Seger[15], Y. Sekiguchi[135], D. Sekihata[135], I. Selyuzhenkov[96,110], S. Senyukov[139], J. J. Seo[63], D. Serebryakov[65], L. Šerkšnytė[108], A. Sevcenco[69], T. J. Shaba[74], A. Shabanov[65], A. Shabetai[117], R. Shahoyan[35], W. Shaikh[112], A. Shangaraev[94], A. Sharma[103], H. Sharma[120], M. Sharma[104], N. Sharma[103], S. Sharma[104], O. Sheibani[127], K. Shigaki[47], M. Shimomura[86], S. Shirinkin[95], Q. Shou[41], Y. Sibiriak[91], S. Siddhanta[56], T. Siemiarczuk[88], T. F. Silva[123], D. Silvermyr[83], G. Simonetti[35], B. Singh[108], R. Singh[89], R. Singh[104], R. Singh[51], V. K. Singh[143], V. Singhal[143], T. Sinha[112], B. Sitar[13], M. Sitta[32], T. B. Skaali[20], G. Skorodumovs[107], M. Slupecki[45], N. Smirnov[148], R. J. M. Snellings[64], C. Soncco[114], J. Song[127], A. Songmoolnak[118], F. Soramel[28], S. Sorensen[133], I. Sputowska[120], J. Stachel[107], I. Stan[69], P. J. Steffanic[133], S. F. Stiefelmaier[107], D. Stocco[117], I. Storehaug[20], M. M. Storetvedt[37], C. P. Stylianidis[93], A. A. P. Suaide[123], T. Sugitate[47], C. Suire[80], M. Suljic[35], R. Sultanov[95], M. Šumbera[98], V. Sumberia[104], S. Sumowidagdo[52], S. Swain[67], A. Szabo[13], I. Szarka[13], U. Tabassam[14], S. F. Taghavi[108], G. Taillepied[137], J. Takahashi[124], G. J. Tambave[21], S. Tang[7,137], Z. Tang[131], M. Tarhini[117], M. G. Tarzila[49], A. Tauro[35], G. Tejeda Muñoz[46], A. Telesca[35], L. Terlizzi[25], C. Terrevoli[127], G. Tersimonov[3], S. Thakur[143], D. Thomas[121], R. Tieulent[138], A. Tikhonov[65], A. R. Timmins[127], M. Tkacik[119], A. Toia[70], N. Topilskaya[65], M. Toppi[53], F. Torales-Acosta[19], T. Tork[80], S. R. Torres[38], A. Trifiró[33,57], S. Tripathy[55,71], T. Tripathy[50], S. Trogolo[28,35], G. Trombetta[34], V. Trubnikov[3], W. H. Trzaska[128], T. P. Trzcinski[144], B. A. Trzeciak[38], A. Tumkin[111], R. Turrisi[58], T. S. Tveter[20], K. Ullaland[21], A. Uras[138], M. Urioni[59,142], G. L. Usai[23], M. Vala[39], N. Valle[29,59], S. Vallero[61], N. van der Kolk[64], L. V. R. van Doremalen[64], M. van Leeuwen[93], P. Vande Vyvre[35], D. Varga[147], Z. Varga[147], M. Varga-Kofarago[147], A. Vargas[46], M. Vasileiou[87], A. Vasiliev[91], O. Vázquez Doce[108], V. Vechernin[115], E. Vercellin[25], S. Vergara Limón[46], L. Vermunt[64], R. Vértesi[147], M. Verweij[64], L. Vickovic[36], Z. Vilakazi[134], O. Villalobos Baillie[113], G. Vino[54], A. Vinogradov[91], T. Virgili[30], V. Vislavicius[92], A. Vodopyanov[77], B. Volkel[35], M. A. Völkl[107], K. Voloshin[95], S. A. Voloshin[145], G. Volpe[34], B. von Haller[35], I. Vorobyev[108], D. Voscek[119], J. Vrláková[39], B. Wagner[21], C. Wang[41], D. Wang[41], M. Weber[116], R. J. G. V. Weelden[93], A. Wegrzynek[35], S. C. Wenzel[35], J. P. Wessels[146], J. Wiechula[70], J. Wikne[20], G. Wilk[88], J. Wilkinson[110], G. A. Willems[146], B. Windelband[107], M. Winn[140], W. E. Witt[133], J. R. Wright[121], W. Wu[41], Y. Wu[131], R. Xu[7], S. Yalcin[79], Y. Yamaguchi[47], K. Yamakawa[47], S. Yang[21], S. Yano[47,140], Z. Yin[7], H. Yokoyama[64], I.-K. Yoo[17], J. H. Yoon[63], S. Yuan[21], A. Yuncu[107], V. Zaccolo[24], A. Zaman[14], C. Zampolli[35], H. J. C. Zanoli[64], N. Zardoshti[35], A. Zarochentsev[115], P. Závada[68], N. Zaviyalov[111], H. Zbroszczyk[144], M. Zhalov[101], S. Zhang[41], X. Zhang[7], Y. Zhang[131], V. Zherebchevskii[115], Y. Zhi[11], D. Zhou[7], Y. Zhou[92], J. Zhu[7,110], Y. Zhu[7], A. Zichichi[26], G. Zinovjev[3], N. Zurlo[59,142]

[1] A.I. Alikhanyan National Science Laboratory (Yerevan Physics Institute) Foundation, Yerevan, Armenia
[2] AGH University of Science and Technology, Cracow, Poland
[3] Bogolyubov Institute for Theoretical Physics, National Academy of Sciences of Ukraine, Kiev, Ukraine
[4] Department of Physics and Centre for Astroparticle Physics and Space Science (CAPSS), Bose Institute, Kolkata, India
[5] Budker Institute for Nuclear Physics, Novosibirsk, Russia
[6] California Polytechnic State University, San Luis Obispo, CA, USA
[7] Central China Normal University, Wuhan, China
[8] Centro de Aplicaciones Tecnológicas y Desarrollo Nuclear (CEADEN), Havana, Cuba
[9] Centro de Investigación y de Estudios Avanzados (CINVESTAV), Mexico City and Mérida, Mexico
[10] Chicago State University, Chicago, IL, USA
[11] China Institute of Atomic Energy, Beijing, China
[12] Chungbuk National University, Cheongju, Republic of Korea
[13] Faculty of Mathematics, Physics and Informatics, Comenius University Bratislava, Bratislava, Slovakia
[14] COMSATS University Islamabad, Islamabad, Pakistan
[15] Creighton University, Omaha, NE, USA
[16] Department of Physics, Aligarh Muslim University, Aligarh, India
[17] Department of Physics, Pusan National University, Pusan, Republic of Korea
[18] Department of Physics, Sejong University, Seoul, Republic of Korea
[19] Department of Physics, University of California, Berkeley, CA, USA
[20] Department of Physics, University of Oslo, Oslo, Norway
[21] Department of Physics and Technology, University of Bergen, Bergen, Norway

[22] Dipartimento di Fisica dell'Università 'La Sapienza' and Sezione INFN, Rome, Italy
[23] Dipartimento di Fisica dell'Università and Sezione INFN, Cagliari, Italy
[24] Dipartimento di Fisica dell'Università and Sezione INFN, Trieste, Italy
[25] Dipartimento di Fisica dell'Università and Sezione INFN, Turin, Italy
[26] Dipartimento di Fisica e Astronomia dell'Università and Sezione INFN, Bologna, Italy
[27] Dipartimento di Fisica e Astronomia dell'Università and Sezione INFN, Catania, Italy
[28] Dipartimento di Fisica e Astronomia dell'Università and Sezione INFN, Padua, Italy
[29] Dipartimento di Fisica e Nucleare e Teorica, Università di Pavia, Pavia, Italy
[30] Dipartimento di Fisica 'E.R. Caianiello' dell'Università and Gruppo Collegato INFN, Salerno, Italy
[31] Dipartimento DISAT del Politecnico and Sezione INFN, Turin, Italy
[32] Dipartimento di Scienze e Innovazione Tecnologica dell'Università del Piemonte Orientale and INFN Sezione di Torino, Alessandria, Italy
[33] Dipartimento di Scienze MIFT, Università di Messina, Messina, Italy
[34] Dipartimento Interateneo di Fisica 'M. Merlin' and Sezione INFN, Bari, Italy
[35] European Organization for Nuclear Research (CERN), Geneva, Switzerland
[36] Faculty of Electrical Engineering, Mechanical Engineering and Naval Architecture, University of Split, Split, Croatia
[37] Faculty of Engineering and Science, Western Norway University of Applied Sciences, Bergen, Norway
[38] Faculty of Nuclear Sciences and Physical Engineering, Czech Technical University in Prague, Prague, Czech Republic
[39] Faculty of Science, P.J. Šafárik University, Košice, Slovakia
[40] Frankfurt Institute for Advanced Studies, Johann Wolfgang Goethe-Universität Frankfurt, Frankfurt, Germany
[41] Fudan University, Shanghai, China
[42] Gangneung-Wonju National University, Gangneung, Republic of Korea
[43] Department of Physics, Gauhati University, Guwahati, India
[44] Helmholtz-Institut für Strahlen- und Kernphysik, Rheinische Friedrich-Wilhelms-Universität Bonn, Bonn, Germany
[45] Helsinki Institute of Physics (HIP), Helsinki, Finland
[46] High Energy Physics Group, Universidad Autónoma de Puebla, Puebla, Mexico
[47] Hiroshima University, Hiroshima, Japan
[48] Zentrum für Technologietransfer und Telekommunikation (ZTT), Hochschule Worms, Worms, Germany
[49] Horia Hulubei National Institute of Physics and Nuclear Engineering, Bucharest, Romania
[50] Indian Institute of Technology Bombay (IIT), Mumbai, India
[51] Indian Institute of Technology Indore, Indore, India
[52] Indonesian Institute of Sciences, Jakarta, Indonesia
[53] INFN, Laboratori Nazionali di Frascati, Frascati, Italy
[54] INFN, Sezione di Bari, Bari, Italy
[55] INFN, Sezione di Bologna, Bologna, Italy
[56] INFN, Sezione di Cagliari, Cagliari, Italy
[57] INFN, Sezione di Catania, Catania, Italy
[58] INFN, Sezione di Padova, Padua, Italy
[59] INFN, Sezione di Pavia, Pavia, Italy
[60] INFN, Sezione di Roma, Rome, Italy
[61] INFN, Sezione di Torino, Turin, Italy
[62] INFN, Sezione di Trieste, Trieste, Italy
[63] Inha University, Incheon, Republic of Korea
[64] Institute for Gravitational and Subatomic Physics (GRASP), Utrecht University/Nikhef, Utrecht, The Netherlands
[65] Institute for Nuclear Research, Academy of Sciences, Moscow, Russia
[66] Institute of Experimental Physics, Slovak Academy of Sciences, Kosice, Slovakia
[67] Institute of Physics, Homi Bhabha National Institute, Bhubaneswar, India
[68] Institute of Physics of the Czech Academy of Sciences, Prague, Czech Republic
[69] Institute of Space Science (ISS), Bucharest, Romania
[70] Institut für Kernphysik, Johann Wolfgang Goethe-Universität Frankfurt, Frankfurt, Germany
[71] Instituto de Ciencias Nucleares, Universidad Nacional Autónoma de México, Mexico City, Mexico
[72] Instituto de Física, Universidade Federal do Rio Grande do Sul (UFRGS), Porto Alegre, Brazil
[73] Instituto de Física, Universidad Nacional Autónoma de México, Mexico City, Mexico

[74] iThemba LABS, National Research Foundation, Somerset West, South Africa
[75] Jeonbuk National University, Jeonju, Republic of Korea
[76] Fachbereich Informatik und Mathematik, Johann-Wolfgang-Goethe Universität Frankfurt Institut für Informatik, Frankfurt, Germany
[77] Joint Institute for Nuclear Research (JINR), Dubna, Russia
[78] Korea Institute of Science and Technology Information, Daejeon, Republic of Korea
[79] KTO Karatay University, Konya, Turkey
[80] Laboratoire de Physique des 2 Infinis, Irène Joliot-Curie, Orsay, France
[81] Laboratoire de Physique Subatomique et de Cosmologie, Université Grenoble-Alpes, CNRS-IN2P3, Grenoble, France
[82] Lawrence Berkeley National Laboratory, Berkeley, CA, USA
[83] Division of Particle Physics, Department of Physics, Lund University, Lund, Sweden
[84] Moscow Institute for Physics and Technology, Moscow, Russia
[85] Nagasaki Institute of Applied Science, Nagasaki, Japan
[86] Nara Women's University (NWU), Nara, Japan
[87] Department of Physics, School of Science, National and Kapodistrian University of Athens, Athens, Greece
[88] National Centre for Nuclear Research, Warsaw, Poland
[89] National Institute of Science Education and Research, Homi Bhabha National Institute, Jatni, India
[90] National Nuclear Research Center, Baku, Azerbaijan
[91] National Research Centre Kurchatov Institute, Moscow, Russia
[92] Niels Bohr Institute, University of Copenhagen, Copenhagen, Denmark
[93] Nikhef, National institute for subatomic physics, Amsterdam, The Netherlands
[94] NRC Kurchatov Institute IHEP, Protvino, Russia
[95] NRC «Kurchatov»Institute-ITEP, Moscow, Russia
[96] NRNU Moscow Engineering Physics Institute, Moscow, Russia
[97] Nuclear Physics Group, STFC Daresbury Laboratory, Daresbury, UK
[98] Nuclear Physics Institute of the Czech Academy of Sciences, Řež u Prahy, Czech Republic
[99] Oak Ridge National Laboratory, Oak Ridge, TN, USA
[100] Ohio State University, Columbus, OH, USA
[101] Petersburg Nuclear Physics Institute, Gatchina, Russia
[102] Physics Department, Faculty of Science, University of Zagreb, Zagreb, Croatia
[103] Physics Department, Panjab University, Chandigarh, India
[104] Physics Department, University of Jammu, Jammu, India
[105] Physics Department, University of Rajasthan, Jaipur, India
[106] Physikalisches Institut, Eberhard-Karls-Universität Tübingen, Tübingen, Germany
[107] Physikalisches Institut, Ruprecht-Karls-Universität Heidelberg, Heidelberg, Germany
[108] Physik Department, Technische Universität München, Munich, Germany
[109] Politecnico di Bari and Sezione INFN, Bari, Italy
[110] Research Division and ExtreMe Matter Institute EMMI, GSI Helmholtzzentrum für Schwerionenforschung GmbH, Darmstadt, Germany
[111] Russian Federal Nuclear Center (VNIIEF), Sarov, Russia
[112] Saha Institute of Nuclear Physics, Homi Bhabha National Institute, Kolkata, India
[113] School of Physics and Astronomy, University of Birmingham, Birmingham, UK
[114] Sección Física, Departamento de Ciencias, Pontificia Universidad Católica del Perú, Lima, Peru
[115] St. Petersburg State University, St. Petersburg, Russia
[116] Stefan Meyer Institut für Subatomare Physik (SMI), Vienna, Austria
[117] SUBATECH, IMT Atlantique, Université de Nantes, CNRS-IN2P3, Nantes, France
[118] Suranaree University of Technology, Nakhon Ratchasima, Thailand
[119] Technical University of Košice, Kosice, Slovakia
[120] The Henryk Niewodniczanski Institute of Nuclear Physics, Polish Academy of Sciences, Cracow, Poland
[121] The University of Texas at Austin, Austin, TX, USA
[122] Universidad Autónoma de Sinaloa, Culiacán, Mexico
[123] Universidade de São Paulo (USP), São Paulo, Brazil
[124] Universidade Estadual de Campinas (UNICAMP), Campinas, Brazil

[125] Universidade Federal do ABC, Santo André, Brazil
[126] University of Cape Town, Cape Town, South Africa
[127] University of Houston, Houston, TX, USA
[128] University of Jyväskylä, Jyvaskyla, Finland
[129] University of Kansas, Lawrence, KS, USA
[130] University of Liverpool, Liverpool, UK
[131] University of Science and Technology of China, Hefei, China
[132] University of South-Eastern Norway, Tonsberg, Norway
[133] University of Tennessee, Knoxville, TN, USA
[134] University of the Witwatersrand, Johannesburg, South Africa
[135] University of Tokyo, Tokyo, Japan
[136] University of Tsukuba, Tsukuba, Japan
[137] Université Clermont Auvergne, CNRS/IN2P3, LPC, Clermont-Ferrand, France
[138] Institut de Physique des 2 Infinis de Lyon, Université de Lyon, CNRS/IN2P3, Lyon, France
[139] Université de Strasbourg, CNRS, IPHC UMR 7178, 67000 Strasbourg, France
[140] Départment de Physique Nucléaire (DPhN), Université Paris-Saclay Centre d'Etudes de Saclay (CEA), IRFU, Saclay, France
[141] Università degli Studi di Foggia, Foggia, Italy
[142] Università di Brescia, Brescia, Italy
[143] Variable Energy Cyclotron Centre, Homi Bhabha National Institute, Kolkata, India
[144] Warsaw University of Technology, Warsaw, Poland
[145] Wayne State University, Detroit, MI, USA
[146] Institut für Kernphysik, Westfälische Wilhelms-Universität Münster, Münster, Germany
[147] Wigner Research Centre for Physics, Budapest, Hungary
[148] Yale University, New Haven, CT, USA
[149] Yonsei University, Seoul, Republic of Korea

[a] Also at: Italian National Agency for New Technologies, Energy and Sustainable Economic Development (ENEA), Bologna, Italy
[b] Also at: Dipartimento DET del Politecnico di Torino, Turin, Italy
[c] Also at: D.V. Skobeltsyn Institute of Nuclear Physics, M.V. Lomonosov Moscow State University, Moscow, Russia
[d] Also at: Institute of Theoretical Physics, University of Wroclaw, Wrocław, Poland
[e] Deceased